CHAPTER IV

FINDINGS

4.1 Extraction of *A. paniculata*

Four samples of *A. paniculata* extracts were successfully collected by using several solvents, including n-hexane, dichloromethane (DCM), acetone and methanol. The yield of methanol extracts for both leaves and flowers was the highest at 217 g and 200 g, respectively. Meanwhile, n-hexane extract had the lowest yield compared to the other samples, with 158 g for leaves and 100 g for flowers (Table 4.1).

Table 4.1: A Total Yield (Gram) of *Acmella paniculata* Crude Extract Using Different Solvents.

Extract (crude extract)	Flower (g)	Leaves (g)
n-hexane	100 g	158 g
DCM	150 g	170 g
Acetone	180 g	195 g
Methanol	200 g	217 g

4.2 Growth of Bacteria

S. mutans ATCC 25175 was used in this study. The morphology was confirmed by using Gram staining method. The result showed it is a Gram-positive bacterium with a coccus shaped and grouped in chains (Figure 4.1).

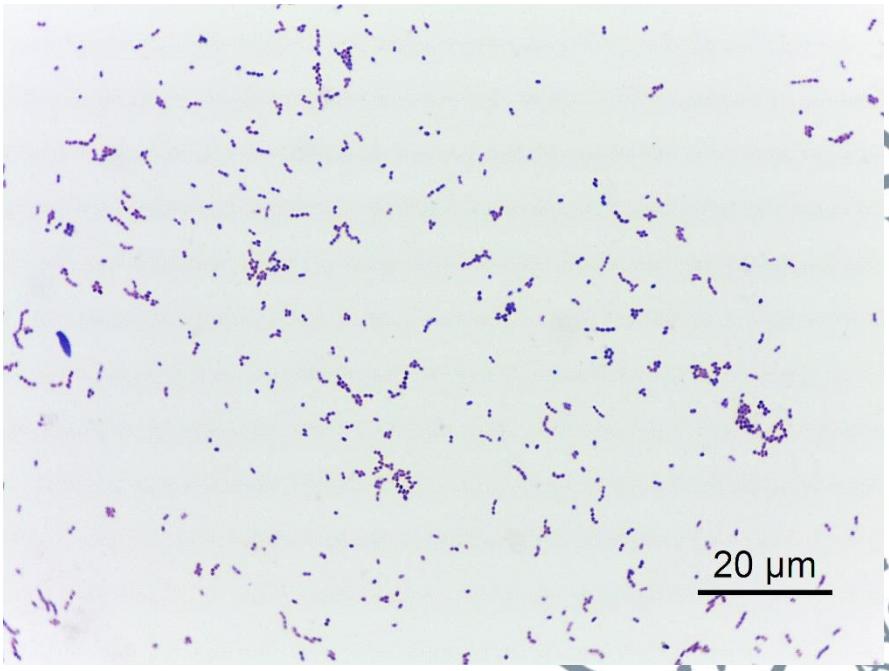

Figure 4.1: Microscopic Depiction of *S. mutans.*

4.3 Antimicrobial Screening of *A. paniculata* Leaves (APL) and *A. paniculata* Flower (APF) Extract by Disc Diffusion Assay

All the variables in Table 4.2 are reported as means with standard deviations. DMSO acted as a negative control, while penicillin represented a positive control. As for leaves extracts, only n-hexane and methanol indicate the presence significance of an inhibition zone from 8.0 mm to 10.0 mm and 7.0 mm to 8.0 mm, respectively when compared to negative control ($p<0.05$). The diameter of the inhibition zone increases as the concentration of the samples for each extract also increases (Figure 4.2).

As for flowers, only n-hexane and dichloromethane (DCM) extracts show significance an inhibition zone from 7.5 mm to 11.3 mm and 9.7 mm to 12.3 mm, respectively when compared to negative control ($p<0.05$). Similar to leaves extracts, as the concentration of the samples for each extract increases, so does the diameter of the

inhibition zone. While the other extracts did not show any changes when compared to the negative control.

Table 4.2: Antibacterial Activity of *A. paniculata* Leaves (APL) and Flower (APF) Crude Extract Towards *S. mutans*. All Values are Represented as Mean ± Standard Deviation. Values on the Same Row with a Different (a, b, c, d) Superscript Letter were Different Significantly with $p < 0.05$. The Zone Diameter of 6.0 ± 0.00 mm was Presented as No Inhibition Activity.

Extract	Sample	Inhibition zone (mm)					
		Concentration (mg/mL)					
		12.5	25	50	100	DMSO (10%)	Penicillin 10U
n-hexane	Leaves	6.0±0.001^{a}	8.0±0.001^{b}	9.0±0.001^{c}	10.0±0.001^{d}	6.0±0.001^{a}	30.0±0.001^{e}
	Flower	7.5±0.5^{a}	8.7±1.15^{b}	10.3±0.57^{c}	11.3±0.57^{d}	6.0±0.001^{a}	30.0±0.001^{e}
DCM	Leaves	6.0±0.001^{a}	6.0±0.001^{a}	6.0±0.001^{a}	6.0±0.001^{a}	6.0±0.001^{a}	30.0±0.001^{e}
	Flower	9.7±0.57^{a}	10.3±1.53^{b}	10.7±2.08^{c}	12.3±2.31^{d}	6.0±0.001^{a}	30.0±0.001^{e}
Acetone	Leaves	6.3±0.6^{a}	6.3±0.6^{a}	6.3±0.6^{a}	6.3±0.6^{a}	6.0±0.001^{a}	30.0±0.001^{e}
	Flower	6.0±0.001^{a}	6.0±0.001^{a}	6.0±0.001^{a}	6.0±0.001^{a}	6.0±0.001^{a}	30.0±0.001^{e}
Methanol	Leaves	6.0±0.001^{a}	6.0±0.001^{a}	7.0±0.001^{b}	8.0±0.001^{c}	6.0±0.001^{a}	30.0±0.001^{e}
	Flower	6.0±0.001^{a}	6.0±0.001^{a}	6.0±0.001^{a}	6.0±0.001^{a}	6.0±0.001^{a}	30.0±0.001^{e}

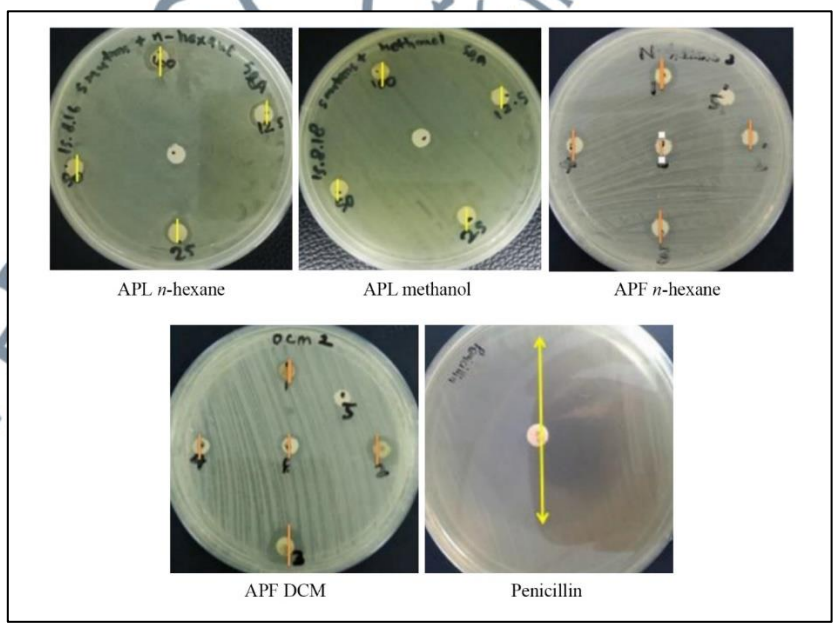

Figure 4.2: Inhibition Zone of *A. paniculata* Extracts and Penicillin against *S. mutans.*

4.4 Minimum Inhibitory Concentration (MIC) and Minimum Bactericidal Concentration (MBC)

Table 4.3 shows the values of MIC and MBC for APL *n*-hexane (APLHE), APL methanol (APLME), APF *n*-hexane (APFHE) and APF DCM (APFDE) extracts. The extracts were chosen based on their antibacterial activity in the disc diffusion assay. The results indicated that the MIC values for APF extracts were lower than those for APL extracts, at 12.5 mg/mL and 25 mg/mL, respectively. The same goes for the value of MBC, 50 mg/mL for both APF extracts, while for APL n-hexane, 50 mg/mL and APL methanol, 100 mg/mL.

Table 4.3: MIC and MBC Value of APLHE, APLME, APFHE and APDE against *S. mutans*. The Values of MIC and MBC for APF Extracts were Lower Compared to APL Extracts.

Extract	MIC (mg/mL)	MBC (mg/mL)
APLHE	25	50
APLME	25	100
APFHE	12.5	50
APFDE	12.5	50
Penicillin	0.008	0.032

4.5 Anti-biofilm Assay

From Figure 4.3, we can see that the percentage of biofilm is 100% without any exposure to *A. paniculata* extracts. However, after being treated at different concentrations, there is a significance different of biofilm formation when compared with the negative control ($p<0.05$). At lower concentrations (6.25 mg/mL) of APL and

APF extracts, the percentage decreased to an average of 11% and 20%, respectively. At higher concentrations (100 mg/mL) of APL and APF extracts, the percentage decreased to an average of 68% and 71%, respectively. The reduction of biofilm formation in *S. mutans* was dose-dependent. The higher concentrations of extracts give the lowest levels of biofilm formation in *S. mutans* (Figure 4.3). However, there is a significant difference in biofilm formation between leaves and flowers at the same concentration ($p<0.05$).

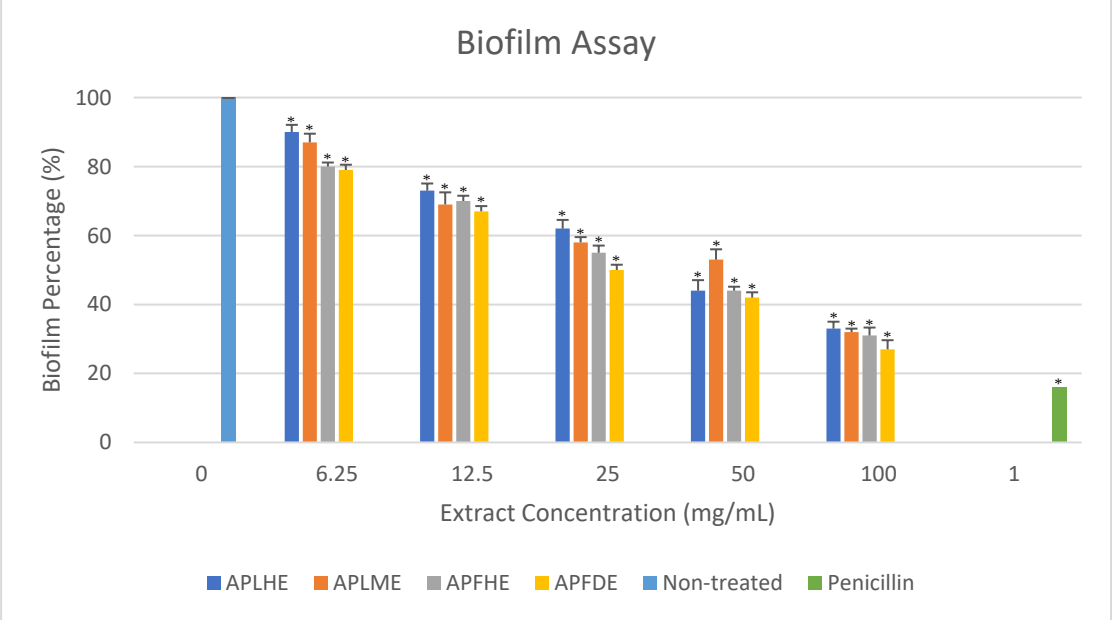

Figure 4.3: Percentage of Biofilm Formation for *S. mutans* Treated with APLHE, APLME, APFHE and APFDE at Concentration (6.25-100 mg/mL) and Penicillin (0.04 mg/mL). All Extracts Show a Significant Difference in Biofilm Formation when Compared to Non-Treated ($p<0.05$).

4.6 Time Kill Assay

Figures 4.4 until 4.8 show the result of the interaction between APLHE, APLME, APFHE, APFDE and penicillin at different concentrations against *S. mutans*

over time. After exposure to the extracts, the growth of *S. mutans* decreases. Figure 4.4 shows the growth of *S. mutans* was significantly reduced ($p<0.05$) more than 3 $\log_{10}$ cfu/mL after being treated with 50 mg/mL (MBC, APLHE) at 24 hours of treatment when compared to non-treated *S. mutans*. Meanwhile, the *S. mutans* when treated with 25 mg/mL (MIC, APLHE) were significantly decreased by less than 3 $\log_{10}$ cfu/mL at 24 hours of treatment ($p<0.05$).

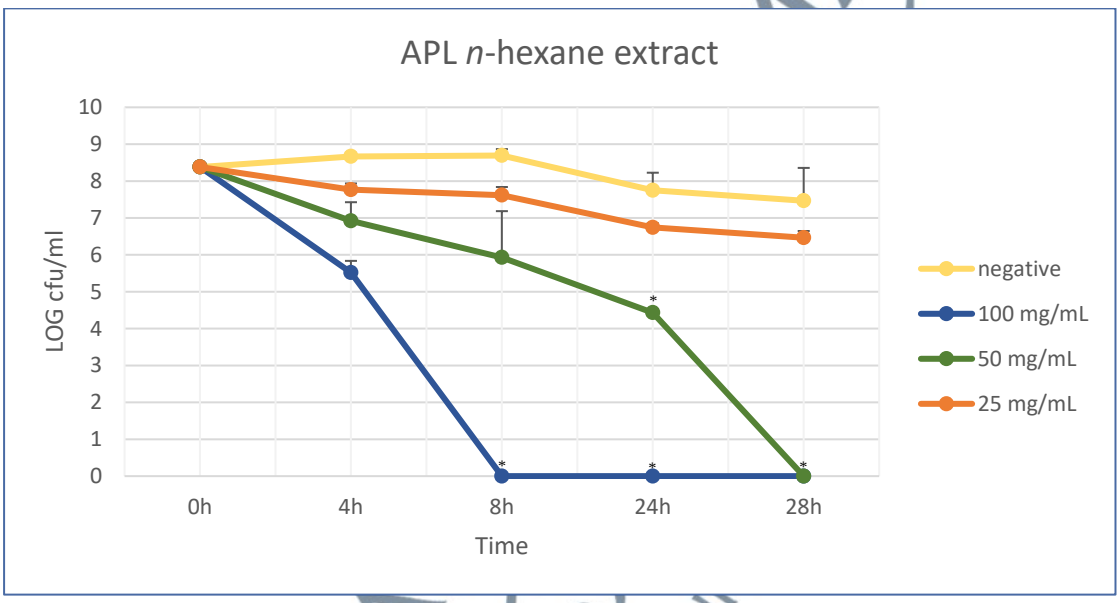

Figure 4.4: The Growth of *S. mutans* ($\log_{10}$ cfu/mL) After Being Treated with APLHE at 0, 4, 8, 24 and 28 Hours. APLHE Treatment at 50 mg/mL and 100 mg/mL Significantly Reduced the Bacteria Growth More Than 3 $\log_{10}$ cfu/mL after 24 Hours and 8 Hours of Treatment, respectively ($p<0.05$). Non-Treated Bacteria Growth Acted as a Negative Control. The Sample was Analysed in Triplicate and Data were Presented as Means ± Standard Deviation.

Figure 4.5 on the other hand, shows that the *S. mutans* were significantly reduced ($p<0.05$) by more than 3 $\log_{10}$ cfu/mL after 24 hours treatments with 25 and 50 mg/mL (MBC and MIC APLME, respectively) when compared with the control. But as for APLME at 100 mg/mL started to show its significant reduction ($p<0.05$) at the early incubation period.

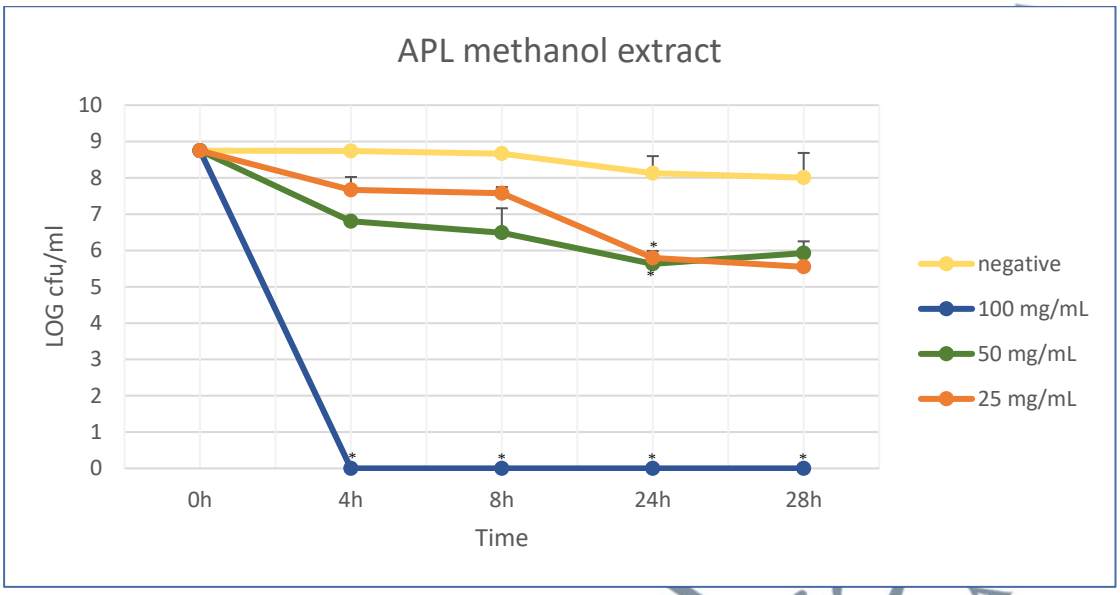

Figure 4.5: The Growth of *S. mutans* (log_{10} cfu/mL) After Being Treated with APLME at 0, 4, 8, 24 and 28 Hours. APLME Treatment at 100 mg/mL Significantly Reduced the Bacteria Growth More Than 3 log_{10} cfu/mL and Kill All the Bacteria at 4 Hours of Treatment ($p<0.05$). While APLME at 25 mg/mL and 50 mg/mL Significantly Reduced the Bacteria Growth More Than 3 log_{10} cfu/mL After 24 Hours of Treatment ($p<0.05$). Non-Treated Bacteria Growth Acted as a Negative Control. The Sample was Analysed in Triplicate and Data were Presented as Means ± Standard Deviation.

As for treatments with APF extracts, Figure 4.6 is the results of treatment with APFHE. The *S. mutans* growth was significantly reduced by more than 3 log_{10} cfu/mL after being treated with 50 mg/mL (MBC, APFHE) for 4 hours ($p<0.05$). Meanwhile, *S. mutans* numbers also showed a significant decrease of less than 3 log_{10} cfu/mL after being treated with 12.5 mg/mL (MIC, APFHE) at 24 hours of treatment ($p<0.05$).

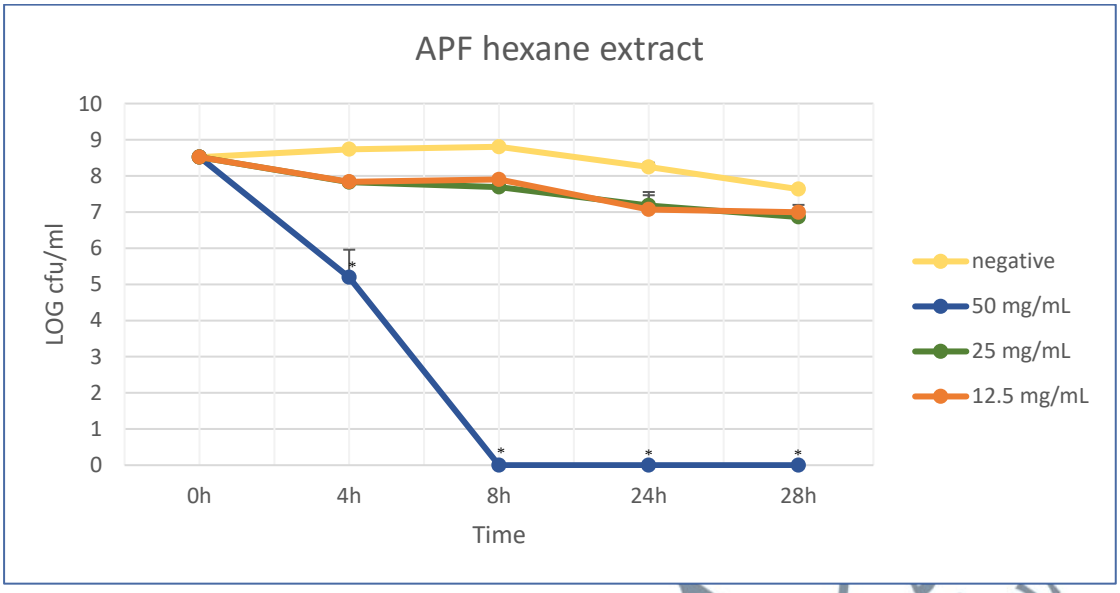

Figure 4.6: The Growth of *S. mutans* (log_{10} cfu/mL) After Being Treated with APFHE at 0, 4, 8, 24 and 28 Hours. APFHE Treatment at 50 mg/mL Significantly Reduced the Bacteria Growth More Than 3 log_{10} cfu/mL at 4 Hours of Treatment ($p<0.05$). Non-Treated Bacteria Growth Acted as a Negative Control. The Sample was Analysed in Triplicate and Data were Presented as Means ± Standard Deviation.

Finally, Figure 4.7 demonstrated that *S. mutans* growth was significantly reduced by more than 3 log_{10} cfu/mL after being treated with 50 mg/mL (APFDE) for 24 hours ($p<0.05$). Meanwhile, *S. mutans* numbers also significantly decreased by less than 3 log_{10} cfu/mL after being treated with 12.5 mg/mL (MIC, APFDE) at 24 hours of treatment ($p<0.05$). Penicillin (0.04 mg/mL) in Figure 4.8 acted as the positive control, and the bacterial concentration decreased by more than 3 log_{10} cfu/mL of cells after 24 hours of treatments ($p<0.05$).

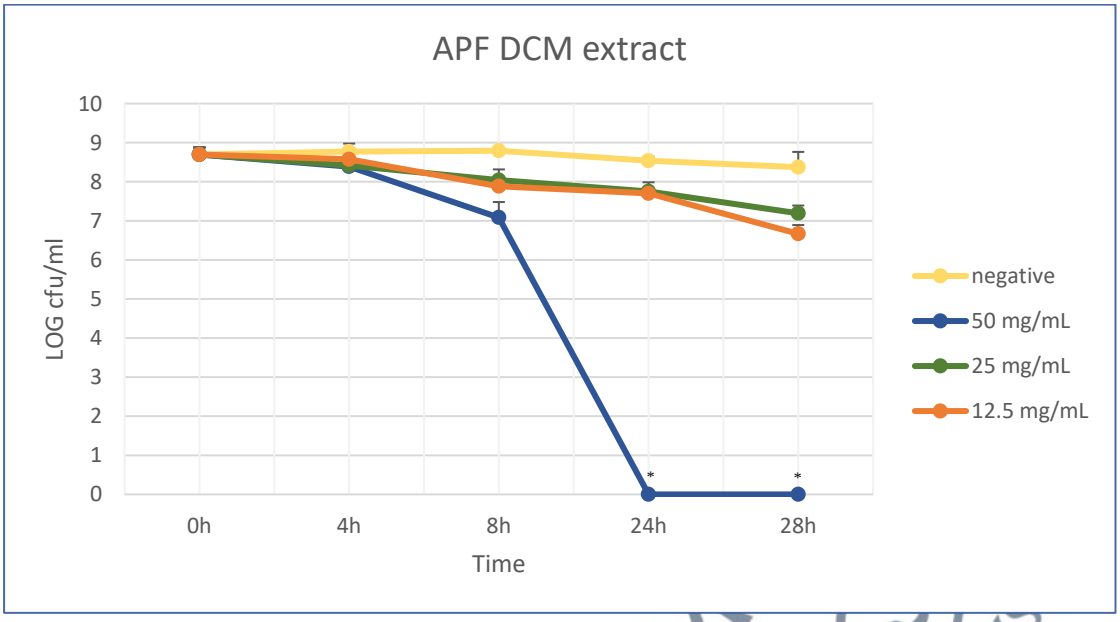

Figure 4.7: The Growth of *S. mutans* (log_{10} cfu/mL) After Being Treated with APFDE at 0, 4, 8, 24 and 28 Hours. APFDE Treatment at 50 mg/mL Significantly Reduced the Bacteria Growth More Than 3 log_{10} cfu/mL at 24 Hours of Treatment ($p<0.05$). Non-Treated Bacteria Growth Acted as a Negative Control. The Sample was Analysed in Triplicate and Data were Presented as Means ± Standard Deviation.

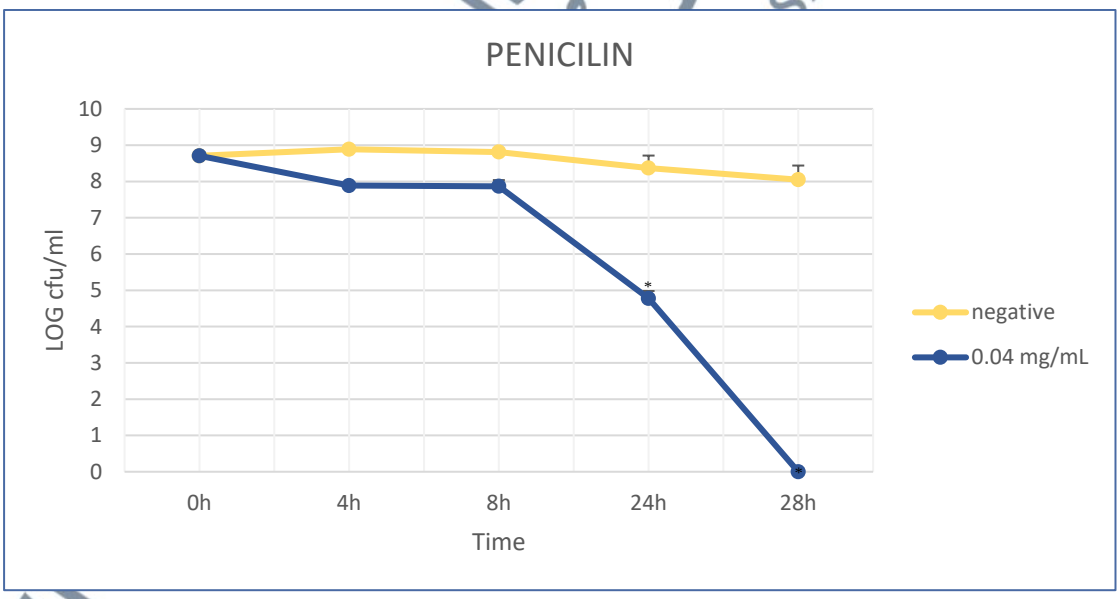

Figure 4.8: The Growth of *S. mutans* (log_{10} cfu/mL) After Being Treated with Penicillin at 0, 4, 8, 24 and 28 Hours. Penicillin Treatment at 0.04 mg/mL Significantly Reduced the Bacteria Growth More Than 3 log_{10} cfu/mL at 24 Hours of Treatment ($p<0.05$). Non-treated Bacteria Growth Acted as a Negative Control. The Sample was Analysed in Triplicate and Data were Presented as Means ± Standard Deviation.

4.7 Scanning Electron Microscope (SEM) Analyses for APFHE and APFDE Treatment against *S. mutans*

Scanning electron microscopy (SEM) and transmission electron microscope (TEM) analysis were carried out to unravel the morphology of *S. mutans* after it was exposed to *A. paniculata* flower extracts for 4 h. SEM and TEM analyses were limited to flower extracts (APFHE and APFDE) because they demonstrated greater antibacterial activity than leaves extracts (APLHE and APLME).

SEM analysis showed the morphology of non-treated *S. mutans* (the control group) was aggregated preferentially within clusters (Figure 4.9 A). The cells are still in coccus shaped and linked together. However, the morphology of *S. mutans* changed after exposure to APFHE at 12.5 mg/mL and 50 mg/mL (Figures 4.9 B and C). The 8000x magnification micrographs of the same culture showed that *S. mutans* cells expanded (E) and then shrank (S). There were also a few holes (H) on the surface, and smaller *S. mutans* cells were observed due to leakage of cytoplasm content. As for *S. mutans* treated with APFDE at 12.5 mg/mL and 50 mg/mL, they were observed to have lysed, wrinkled cell walls and a lack of cytoplasmic content (Figures 4.9 D and E).

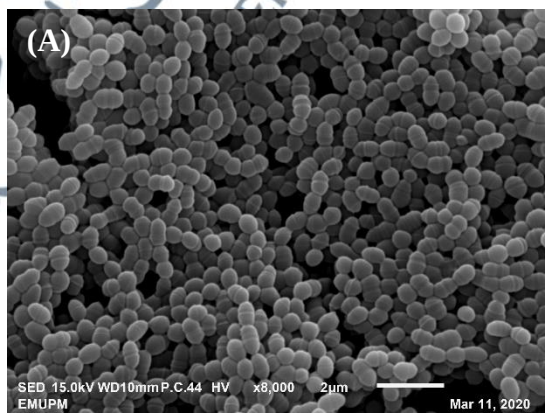

Figure 4.9, continued

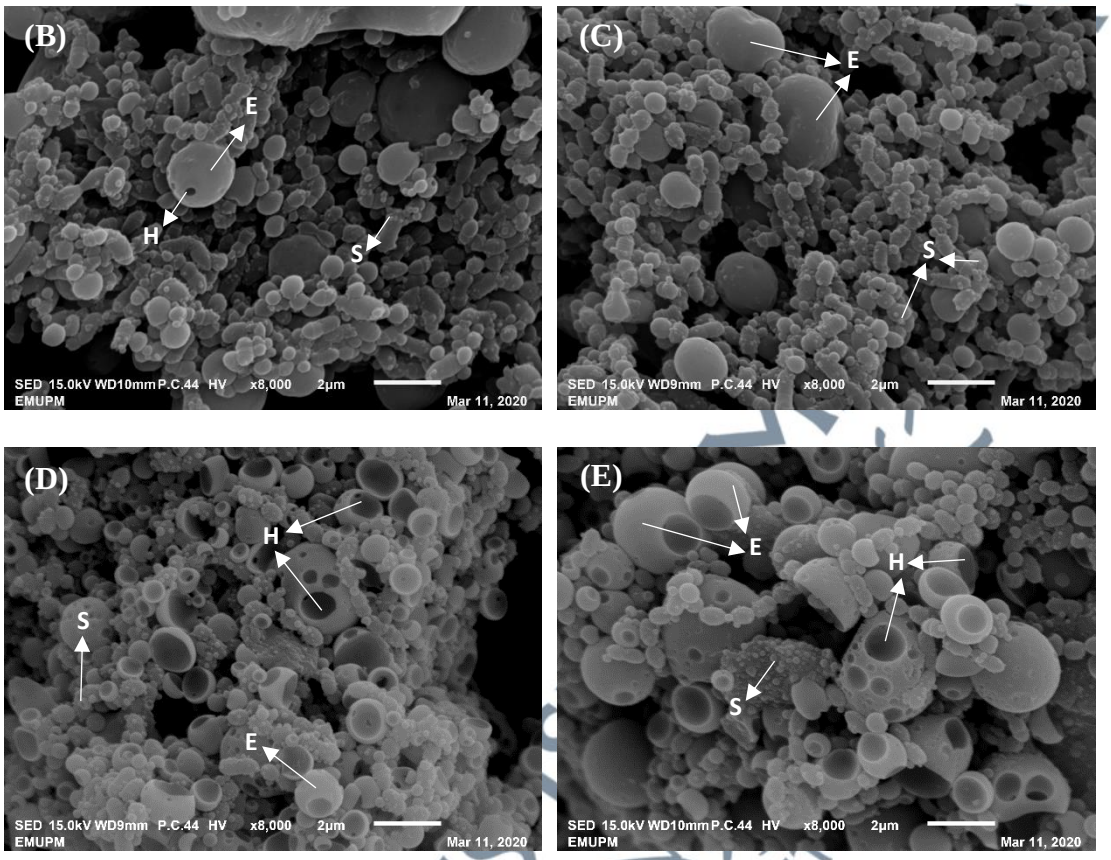

Figure 4.9: SEM Micrograph (8000x Magnification) of (A) Non-Treated *S. mutans*, (B) *S. mutans* Treated with 12.5 mg/mL APFHE, (C) *S. mutans* Treated with 50 mg/mL APFHE, (D) *S. mutans* Treated with 12.5 mg/mL APFDE and (E) *S. mutans* Treated with 50 mg/mL APFDE at 4 Hours.

4.8 Transmission Electron Microscope (TEM) Analyses for APFHE and APFDE Treatment against *S. mutans*

TEM analysis revealed that non-treated *S. mutans* (the control) had bodies with cytoplasm (C), nucleus (N), vacuoles and a membrane (M) that encapsulated the bacterial cell (Figure 4.10 A). TEM micrographs of *S. mutans* treated with APFDE extracts (12.5 and 50 mg/mL) showed cell wall lysis (L), which decreased the cytoplasmic content (Figure 4.10 D and E). Membrane cell disintegration caused by

cytoplasm leakage is an abnormal intracellular reaction of treated bacteria. The coccus shape of *S. mutans* was not conserved and distorted after being treated with APFHE at 12.5 and 50 mg/mL (Figure 4.10 B and C). As a result, treated *S. mutans* showed changes in the peripheral cell surface, hollow formation, and destroyed cell structure.

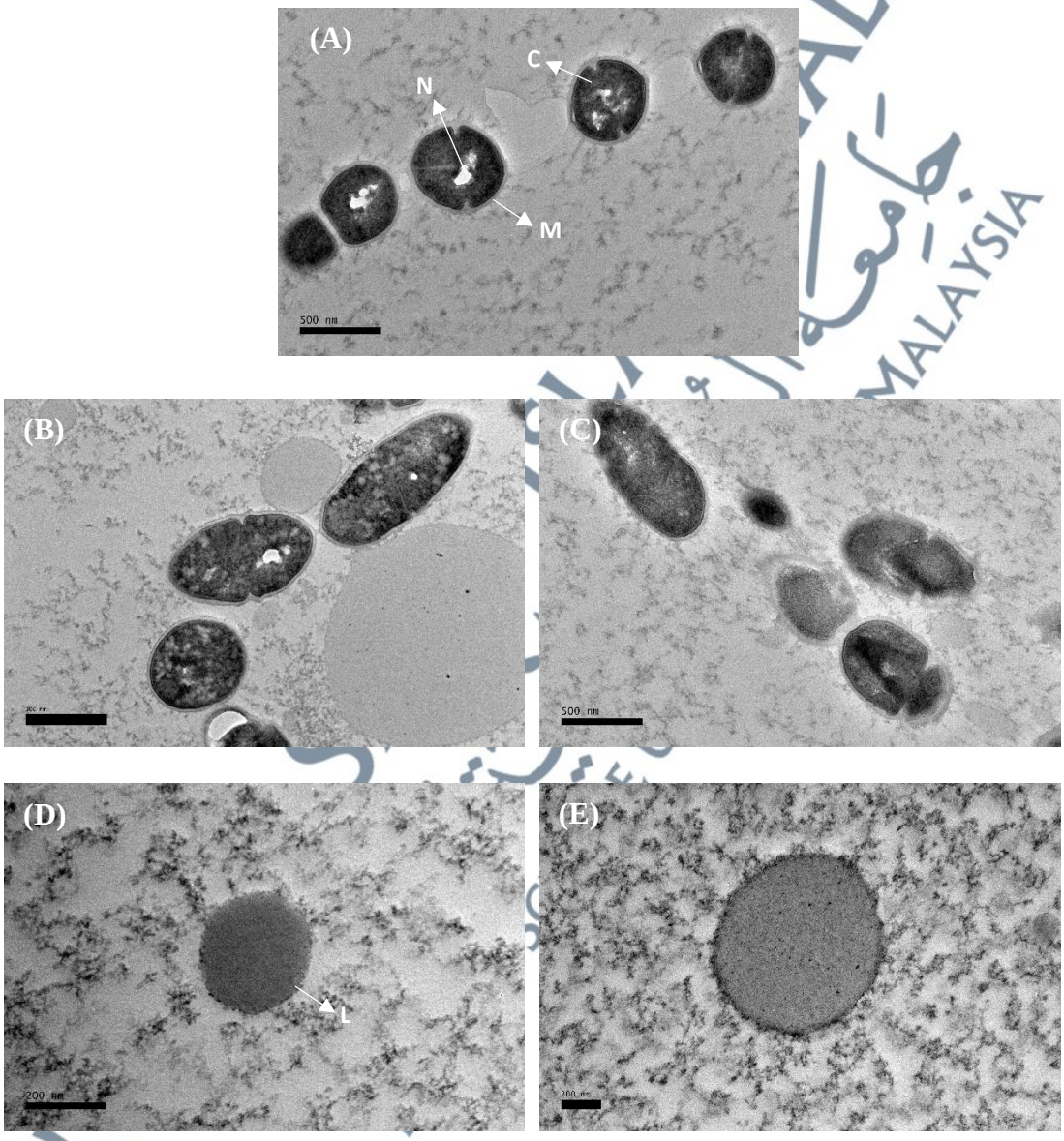

Figure 4.10: TEM Micrograph (8000x – 20000x Magnification) of (A) Non-Treated *S. mutans*, (B) *S. mutans* Treated with 12.5 mg/mL APFHE, (C) *S. mutans* Treated with 50 mg/mL APFHE, (D) *S. mutans* Treated with 12.5 mg/mL APFDE and (E) *S. mutans* Treated with 50 mg/mL APFDE at 4 Hours.

4.9 Gas Chromatography-Mass Spectrometry (GC-MS) Analysis

The bioactive compounds in APFHE and APFDE extracts were identified by GC-MS analysis. The ion chromatograms of APFHE and APFDE extracts were given in Figures 4.11 and 4.12, respectively. The bioactive compounds APFHE and APDHE were given in Tables 4.4 and 4.5, respectively. The chromatogram peaks were integrated and compared to a database of known component spectrums from the GC-MS library. APFHE analysis discovered 22 compounds, including aldehydes, hydrocarbons, fatty acids, and terpenoids. However, fatty acids were found to be the most abundant, with Hexadecanoic acid methyl ester, also known as palmitic acid methyl ester, having the highest peak in the chromatogram (Figure 4.11) and the highest area percentage was n-Hexadecanoic acids, also known as palmitic acid (Table 4.4) (Wang et al., 2018; Trejo et al., 2020). The palmitic acids accounted for 21.81% of the total peak area, suggesting that it may be the major constituent of APFHE, followed by hexadecanoic acid methyl ester (15.64%) and oleic acid (11.73%).

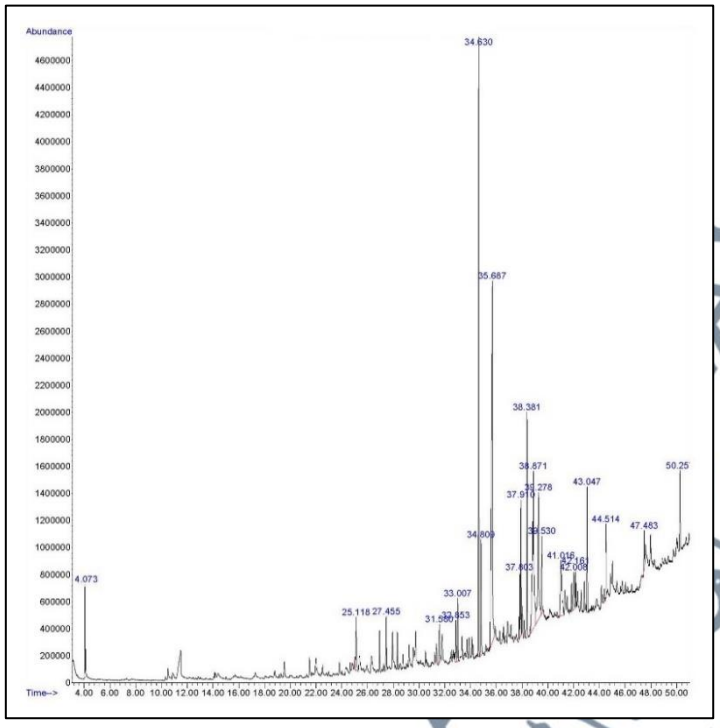

Figure 4.11: Total Ion Chromatogram of the APFHE. The Highest Peak for APFHE was n-Hexadecanoic Acid, Methyl Ester (Retention Time: 34.63).

Table 4.4: GC-MS Analysis of Phytochemical Compounds Identified in APFHE. The Highest Area Percentage for APFHE was n-Hexadecanoic Acid (21.81%).

RT (mins)	Area (%)	Chemical Name	Molecular Formula
4.072	2.36	Hexanal	$C_6H_{12}O$
25.119	1.58	1-Pentadecene	$C_{15}H_{30}$
27.456	1.79	Caryophyllene oxide	$C_{15}H_{24}O$
31.583	1.34	Tetradecanoic acid	$C_{14}H_{28}O_2$
32.854	1.29	Phytol, acetate	$C_{22}H_{42}O_2$
33.005	1.92	5-Methylthiopyridin-2-ol	C_6H_7NOS
34.631	15.64	Hexadecanoic acid, methyl ester	$C_{17}H_{34}O_2$
34.806	3.98	Furan, 2-ethyl-5-methyl-	$C_7H_{10}O$
35.686	21.81	n-Hexadecanoic acid	$C_{16}H_{32}O_2$

Table 4.4, continued

37.802	1.70	9,12-Octadecadienoic acid (Z,Z)-	$C_{18}H_{32}O_2$
37.913	3.49	11-Octadecenoic acid, methyl ester	$C_{19}H_{36}O_2$
38.379	6.29	Methyl stearate	$C_{19}H_{38}O_2$
38.869	11.73	Oleic acid	$C_{18}H_{34}O_2$
39.277	7.26	Octadecanoic acid	$C_{18}H_{36}O_2$
39.533	2.23	Benzene, 1-methoxy-3-(methylthio)-	$C_8H_{10}OS$
41.014	4.13	9-Octadecenal, (Z)-	$C_{18}H_{34}O$
42.011	1.57	5-Hexadecenoic acid, 2-methoxy-	$C_{17}H_{32}O_3$
42.162	1.33	Benzenemethanamine, 2-methyl-	$C_8H_{11}N$
43.048	3.54	Acetamide, N-(2-phenylethyl)-	$C_{10}H_{13}NO$
44.511	1.91	Eicosane	$C_{20}H_{42}$
47.484	0.90	Eicosane	$C_{20}H_{42}$
50.258	2.21	Heptacosane, 1-chloro-	$C_{27}H_{55}Cl$

In terms of APFDE, a total of 16 compounds were found, where fatty acids, particularly octadecanoic acid, appearing to be the most abundant. The compound 9,12-Octadecadienoic acid (Z,Z) also known as Linoleic acid (Manganyi et al., 2019) was detected in the chromatogram at various retention times (RT), and it was also indicated as the highest peak compound at 39.446 minutes (Figure 4.12) with the highest total peak area of 42.41% (Table 4.5).

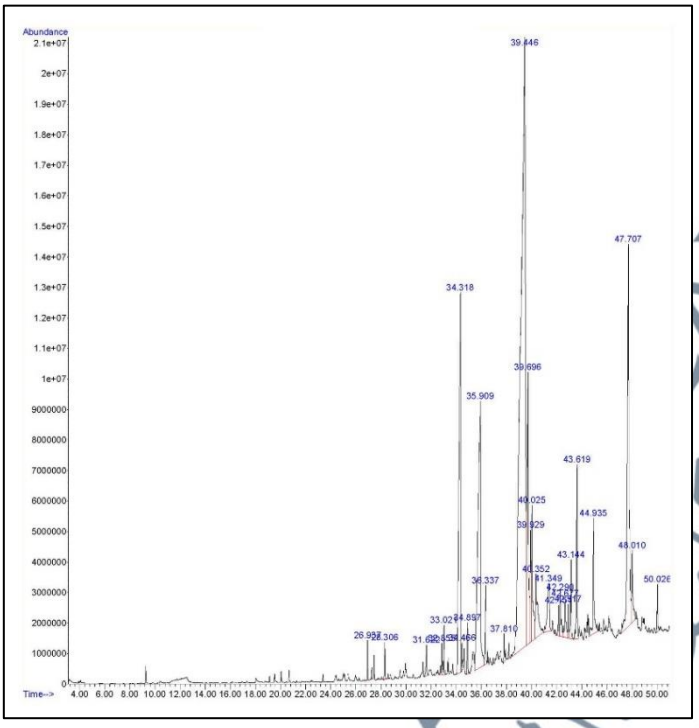

Figure 4.12: Total Ion Chromatogram of the APFDE. The Highest Peak for APFDE was 9,12-Octadecadienoic Acid (Z,Z) (Retention Time: 39.45).

Table 4.5: GC-MS Analysis of Phytochemical Compounds Identified in APFDE. The Highest Area Percentage for APFDE was 9,12-Octadecadienoic Acid (Z,Z) (42.34%).

RT (mins)	Area (%)	Chemical Name	Molecular Formula
31.624	0.39	Tetradecanoic acid	$C_{14}H_{28}O_2$
32.854	0.41	1,19-Eicosadiene	$C_{20}H_{38}$
34.317	9.43	1-Cyclohexene-1-carboxylic acid	$C_7H_{10}O_2$
35.908	11.02	n-Hexadecanoic acid	$C_{16}H_{32}O_2$
37.808	0.34	9,12-Octadecadienoic acid (Z,Z)-	$C_{18}H_{32}O_2$
39.446	42.34	9,12-Octadecadienoic acid (Z,Z)-	$C_{18}H_{32}O_2$
39.697	6.12	Octadecanoic acid	$C_{18}H_{36}O_2$
39.930	1.40	9,12-Octadecadienoic acid (Z,Z)-	$C_{18}H_{32}O_2$
40.349	2.12	4-Fluorobenzoic acid	$C_7H_5FO_2$

Table 4.5, continued

41.346	1.61	9,12-Octadecadienoic acid (Z,Z)-	$C_{18}H_{32}O_2$
42.675	0.84	9,12-Octadecadienoic acid (Z,Z)-	$C_{18}H_{32}O_2$
42.920	0.36	4-Hexenoic acid, 5-hydroxy-3-oxo	$C_8H_{10}O_5$
43.619	2.21	N-(2-Phenylethyl)(2E,6Z,8E)-decatrienamide	$C_{18}H_{23}NO$
44.937	1.90	Hexadecanoic acid, 2-hydroxy-	$C_{16}H_{32}O_3$
47.705	10.38	9,12-Octadecadienoic acid (Z,Z)-	$C_{18}H_{32}O_2$
48.008	1.22	Octadecanoic acid, 2-hydroxy-1-	$C_{18}H_{36}O_3$

4.10 RNA Extraction for *S. mutans* Treated with APFDE

Before collecting gene expression (DEG) data, the RNA was checked for quality because poor-quality RNA can affect gene expression (Vermeulen et al., 2011). Quality RNA has an A260/A280 ratio ~2.0. While RNA with high integrity consists of two bands, namely 23s and 16s with no genomic band (Acosta-Maspons et al., 2019). Therefore, as seen in Figure 4.13 below, the RNA that has been successfully extracted shows that there are two bands. While the optical absorption reading ratio of A260/A280 is approximate to 2.0 (Table 4.6).

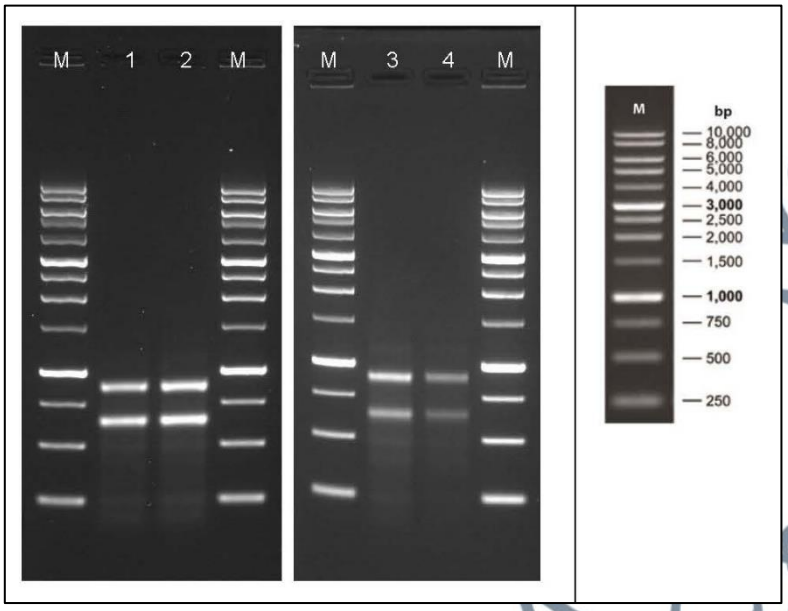

Figure 4.13: DNA Extraction Profile of *S. mutans* Treated with APFDE (MBC) that been Analysed Using Nano-Drop Analysis. Well (1) and (2) were Non-Treated *S. mutans* while Well (3) and (4) were *S. mutans* Treated with APFDE. (M) is the 1 kb DNA Ladder Marker.

Table 4.6: Nanodrop Analysis RNA Isolated from Untreated and Treated *S. mutans*. (Absorption Values 260/280 and 260/230 Indicate Nucleic Acid Purity). Nucleic Acid Purity is Defined as 260/280 Absorption Values Ranging from 1.9 to 2.0 and 260/230 Absorption Values Ranging from 2.0 to 2.2.

Num.	Sample Name	RNA Extraction (ng/µL)	A260/280	A260/230
1	Non-treated SM (control 1)	117.36	2.219	1.135
2	Non-treated SM (control 2)	149.52	2.236	1.227
3	SM treated with APFDE (Treated 1)	82.20	2.207	1.136
4	SM treated with APFDE (Treated 2)	65.20	2.210	1.210

4.11 Transcriptomic Profile Analysis

4.11.1 Mapping to Reference Genome

The mapping algorithm was chosen based on the characteristics of the reference genome. Bowtie2 was chosen for genomes of bacteria and other species with high gene density in general. The mismatch parameter was set to two, and the rest of the parameters were set to default. If there is no contamination and the correct reference genome is chosen, the total mapped rate should be greater than 70% and the percentage of reads that can be mapped to multiple sites in the reference genome should be less than 10%.

Table 4.7: Mapping Analysis of Non-Treated and Treated *S. mutans* genome. The Genome of Smunn2025 had been Used as Reference Genome.

Sample Name	Treated1 APFDE	Treated2 APFDE	Non-treated	Non-treated
Total reads	16016284	19238986	15934552	19460034
Total mapped reads	15305549	18469977	15447751	18883637
Uniquely mapped reads	14894816	17318063	15093404	18584375
Multiple mapped reads	410733	1151914	354347	299262
Total mapping rate	95.56%	96%	96.94%	97.04%
Uniquely mapping rate	93%	90.02%	94.72%	95.50%
Multiple mapping rate	2.56%	5.99%	2.22%	1.54%

4.11.2 Expression Quantification

Gene expression level was measured by transcript abundance. The greater the abundance, the higher the gene expression level. In our RNA-seq analysis, the gene expression level is estimated by counting the reads that map to genes or exons. The read

count is not only proportional to the actual gene expression level but is also proportional to the gene length and the sequencing depth. For the gene expression levels estimated from different genes and experiments to be comparable, the FPKM was used. In RNA-seq, the expected number of fragments per kilobase of transcript sequence per million base pair-sequenced (FPKM) is the most commonly used method of estimating gene expression levels, taking into account the effects of sequencing depth and gene length on fragment counting (Abbas-Aghababazadeh & Fridley, 2018; Zhao et al., 2021).

Feature Counts software was used to analyse the gene expression levels in this experiment. The result files present the number of genes with different expression levels and the expression level of single genes (Table 4.8). In general, an FPKM value of 0.1 or 1 is set as the threshold for determining whether the gene is expressed or not.

Table 4.8: The Number of Genes with Different Expression Levels.

FPKM Interval	Control 1	Control 2	Treated 1	Treated 2
0 ~ 1	266 (12.33%)	266 (12.33%)	259 (12%)	255 (11.82%)
1 ~ 3	27 (1.25%)	25 (1.16%)	18 (0.83%)	17 (0.79%)
3 ~ 15	142 (6.58%)	134 (6.21%)	79 (3.66%)	63 (2.92%)
15 ~ 60	352 (16.31%)	341 (15.8%)	259 (12%)	248 (11.49%)
> 60	1371 (63.53%)	1392 (64.5%)	1543 (71.5%)	1575 (72.98%)

4.11.3 RNA-seq Advanced QC

In this project, all the samples were greater than 0.92, with the treated at 0.982 and the control at 0.985. This value is closer to 1, indicating a strong positive correlation, implying that these samples are very similar.

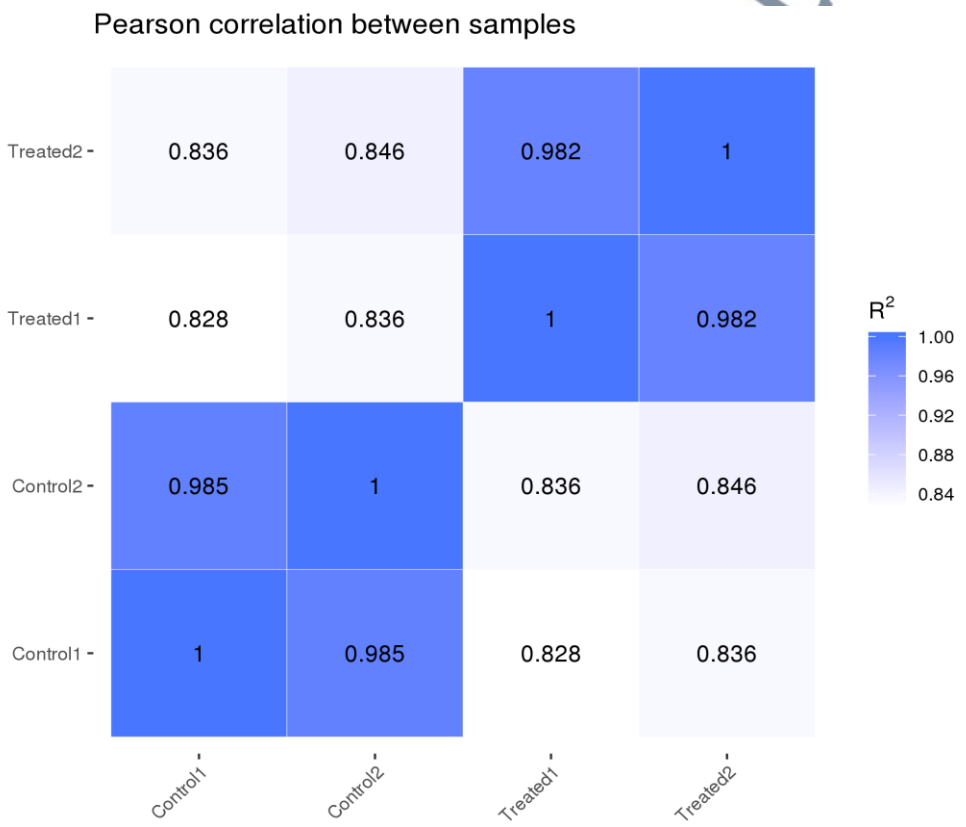

Figure 4.14: Correlation of RNA-seq Samples.

4.11.4 Differential of Sequencing Gene (DEG)

RNA sequence analysis showed that APFDE has significant ($p<0.05$) effects on the transcriptomic profile of *S. mutans* compared to control. From 1266 genes, 622 genes were downregulated and 644 genes were upregulated (Figure 4.15).

Same as in the volcano plot, which was used to identify specific genes with high fold changes and statistical significance in gene expression changes. Figure 4.16 displays the volcano plot results. Genes that were significantly different are highlighted in red as upregulated and green as downregulated, indicating that a total of 644 genes were upregulated and 622 genes were downregulated.

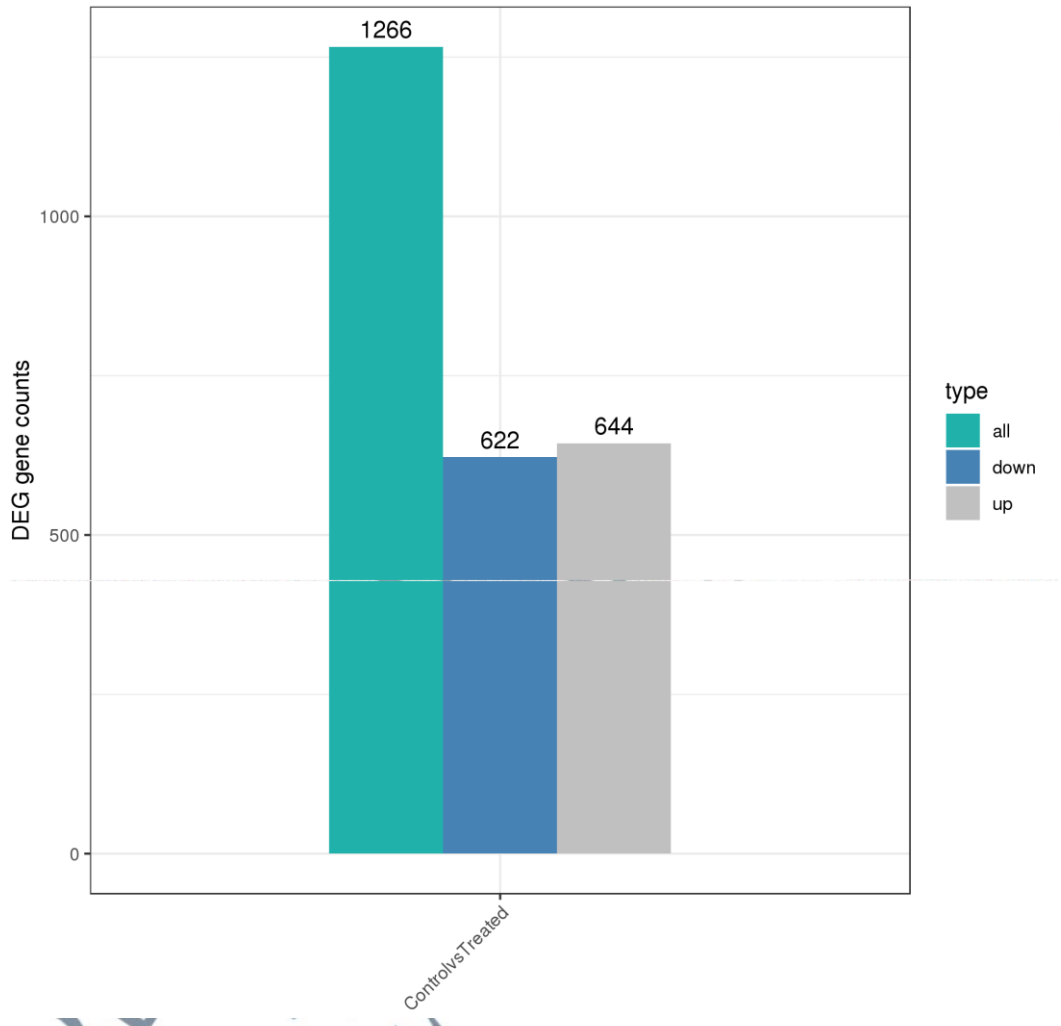

Figure 4.15: Total DEG of *S. mutans* After APFDE Treatment. There are 1266 Genes in Total, with 622 Downregulated and 644 Upregulated.

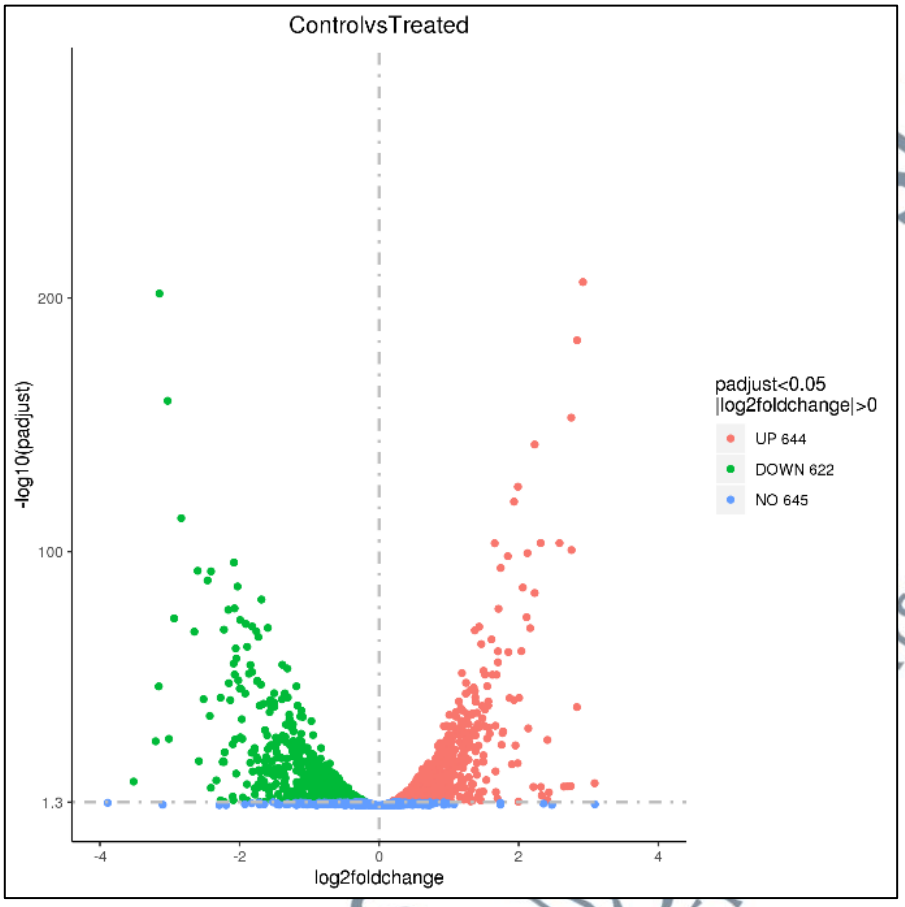

Figure 4.16: Image of a Volcano Depicting Gene Regulation in *S. mutans* Treated with APFD (MIC). Downregulated Genes are Represented by Green, while Upregulated Genes are Represented by Red.

4.11.5 Downregulated Genes

Table 4.9 showed the differential gene expression regulation of *S. mutans* treated with APFDE. The differential regulated gene had been done by comparing to non-treated bacteria. In downregulated genes, several pathways involved when *S. mutans* treated with APFDE. Table 4.9 (A) showed genes of DNA replication and peptidoglycan synthesis were downregulated after treatment such as *murC* and *murD* (peptidoglycan synthesis) and *ssb* and *dnaG* (DNA replication).

Table 4.9 (A): DNA Replication Genes (*SmuNN2025_1359, ssb, dnaG, rnh3* and *hol b*) and Peptidoglycan Biosynthesis Genes (*murD, uppS, murC2, pbp2b, murE, murN* and *murB*) were Downregulated After Treated with APFDE.

Gene Name	Log_2 Fold-change	P value	Gene Description
SmuNN2025_1359	-1.6044657	2.09E-29	DNA polymerase III, delta subunit
ssb	-0.6788083	1.88E-14	putative single-stranded DNA-binding protein
dnaG	-0.5734505	3.44E-11	DNA primase catalytic core, N-terminal domain
rnh3	-0.3960807	0.00051026	putative ribonuclease PF01351: Ribonuclease HII
holB	-0.3897243	0.00139286	putative DNA polymerase III delta subunit &&
murD	-0.855528	1.69E-14	putative D-glutamic acid adding enzyme
uppS	-1.1305843	1.94E-14	putative undecaprenyl pyrophosphate synthetase
murC2	-0.7820073	1.92E-11	putative UDP-N-acetylmuramyl tripeptide synthetase
pbp2b	-0.5783955	4.89E-09	Penicillin-binding Protein dimerisation domain
murE	-0.4486175	3.23E-05	putative UDP-N-acetylmuramoylananine-D-glutamate-
murN	-0.403607	0.00089	putative peptidoglycan branched peptide synthesis protein
murB	-0.440412	0.002353	putative UDP-N-acetylenolpyruvoylglucosamine reductase

Table 4.9 (B) showed genes of citrate cycle were downregulated after *S. mutans* exposed with APFDE, such as *idh, Cit B and Cit Z.*

Table 4.9 (B): Citrate Cycle Pathway (Downregulated).

Gene Name	Log_2 Fold-change	P value	Gene Description
idh	-1.1609763	1.03E-06	isocitrate dehydrogenase
Cit b	-1.9680369	1.02E-34	aconitate hydratase
Cit z	-1.5699562	1.40E-08	citrate synthase

Table 4.9 (C) showed genes of glycolysis pathway was downregulated after *S. mutans* exposed with APFDE.

Table 4.9 (C): Glycolysis (*SmuNN2025_0739*) and Pyruvate Metabolism (*pmgY)* (Downregulated).

Gene Name	Log_2 Fold-change	P value	Gene Description
pmgY	-1.3143487	3.10E-56	phosphoglyceromutase
SmuNN2025_0739	-1.0363445	1.96E-13	conserved hypothetical protein & PF00753: Metallo-beta-lactamase superfamily

Table 4.9 (D) showed genes of biofilm and quorum sensing were downregulated after treatment such as *gtfB*, *gtfC* and *brpA.*

Table 4.9 (D): Biofilm and Quorum Sensing Genes (Downregulated).

Gene Name	Log_2 Fold-change	P value	Gene Description
gtfB	-1.61	2.09E-29	Glucosyltransferase-I
gtfC	-1.18	1.03E-06	Glucosyltransferase-SI
gbpB	-0.60	1.88E-14	Glucan Binding Protein B
brpA	-0.43	3.23E-05	Transcriptional Regulator
comD	-0.42	0.002353	Histidine kinase
comE	-1.00	1.96E-13	Response regulator ComE
ftsA	-0.38	0.00139286	FtsA Protein
ftsL	-0.81	1.94E-14	Cell Division Protein
ftsW	-1.09	1.06E-06	FtsW protein
CovR	-0.38	0.00139286	CovR protein
rpsR	-0.32	0.00089	30S Ribosomal protein
rpmC	-0.29	0.0004389	50S Ribosomal protein
dltA	-0.49	0.004890	D-alanine-D-alanyl carrier protein ligase

4.11.6 Upregulated Genes

Table 4.10 showed Log_2 fold change of upregulated genes in *S. mutans* treated with APFDE. All of the genes involved in microbial metabolism in diverse environments (KEGG pathway).

Table 4.10: Log_2 Fold Change of Upregulated Genes in *S. mutans* Exposed in APFDE.

Gene Name	Log_2 Fold-change	P value	Gene Description
pdhD	2.8355	1.30E-186	putative dihydrolipoamide dehydrogenase
pf1	2.2289	2.37E-145	pyruvate formate-lyase
pdhA	2.5844	2.45E-106	putative pyruvate dehydrogenase E1 component alpha subunit
SmuNN2025_1677	2.0384	3.69E-63	Beta-lactamase superfamily domain
glk	1.1948	2.12E-34	putative glucose kinase
ldh	0.9586	3.00E-33	lactate dehydrogenase
serA	0.3443	0.0001	putative D-3-phosphoglycerate dehydrogenase

4.11.7 Cluster Analysis of Gene Expression Differences.

Cluster analysis was used to identify genes with similar expression patterns under different experimental conditions. It may be possible to deduce the unknown functions of previously characterised genes or the function of unknown genes by clustering genes with similar expression patterns. In hierarchical clustering, different coloured areas denote different groups (clusters) of genes, and genes within each cluster may have similar functions or participate in the same biological process (Figure 4.17).

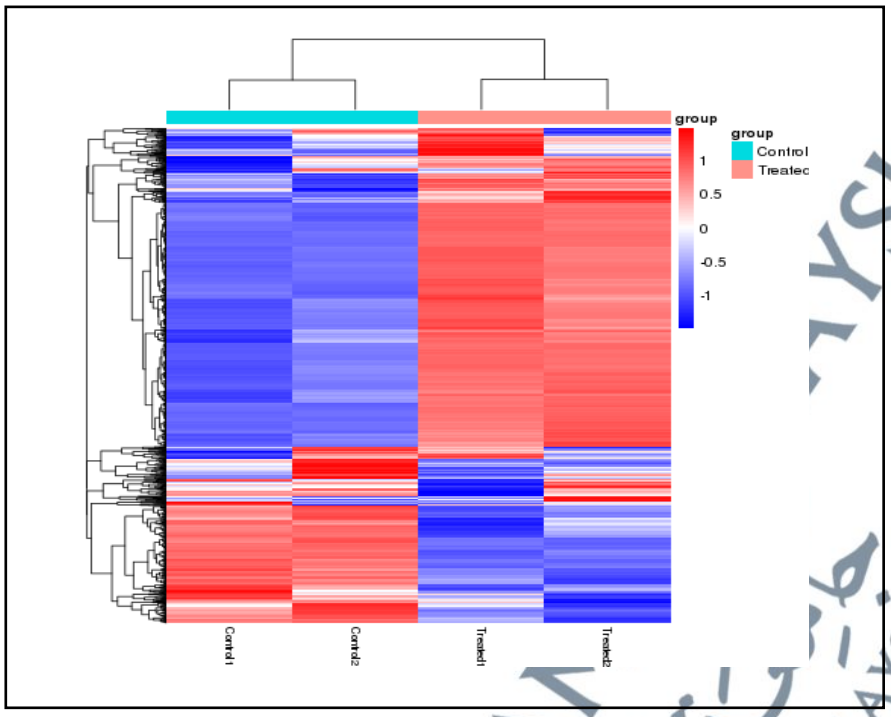

Figure 4.17: Upper Panel: Overall FPKM Cluster Analysis Results, Clustered Using the Log_2 (FPKM+1) Value. Genes With High Expression Levels are Indicated in Red, while Genes with Low Expression Levels are Indicated in Blue. The Colour Spectrum from Red to Blue Represents the Log_2 (FPKM+1) Value from Large to Small. Lower Panel: Line Chart of Log_2 (FPKM+1). A Subline Chart's Grey Lines Represent the Relative Expression Value of a Gene Cluster Under Different Experimental Conditions, while the Blue Line Represents the Mean Value. The x-axis Represents the Experimental Condition, While the y-Axis Represents the Relative Expression Level.

4.11.8 Gene Ontology

The GO categories among DEG were shown in Figure 4.18-4.20. It was divided into three sections: cellular components, molecular function, and biological processes. GO terms with padj < 0.05 were regard as significant enrichment. In molecular function (MF), about 20 categories were downregulated and nucleic acid binding of molecular function was higher compared to other categories (Figure 4.18). Meanwhile, genes involved in the binding process were the most downregulated after being treated with APFDE. In cellular components, about 19 components were downregulated after *S. mutans* was treated with APFDE (Figure 4.19). The cytoplasmic component was the

most downregulated after being treated with APFDE. About 524 genes of cellular components were downregulated in this analysis. Gene expression, RNA processing, and macromolecular metabolic processes were the most enriched biology process for downregulated DEG in the presence of APFDE (Figure 4.20). The most downregulated genes were involved in the biological process and cellular component.

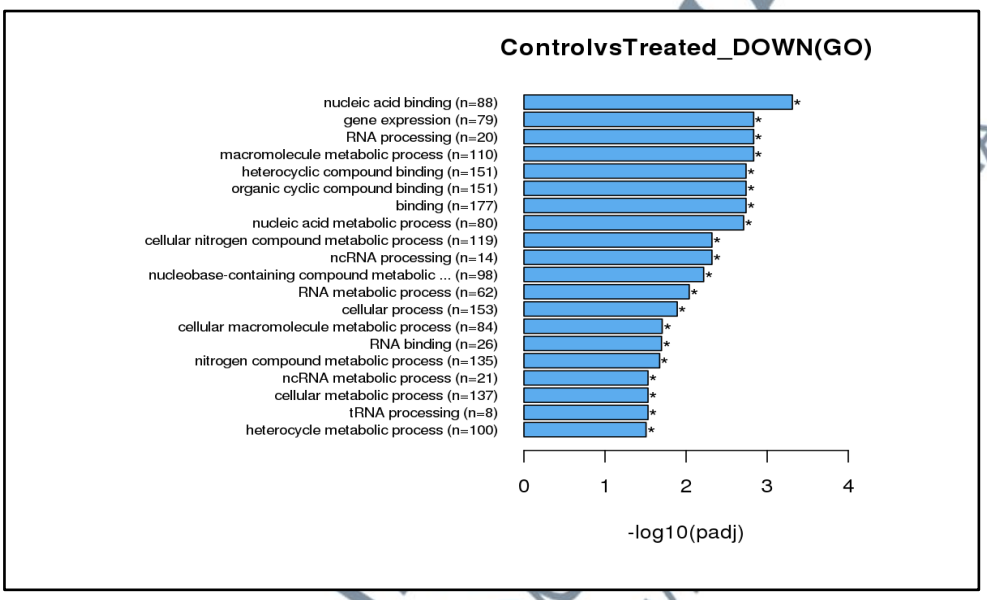

Figure 4.18: Gene Ontology Category of DEGs in Molecular Function.

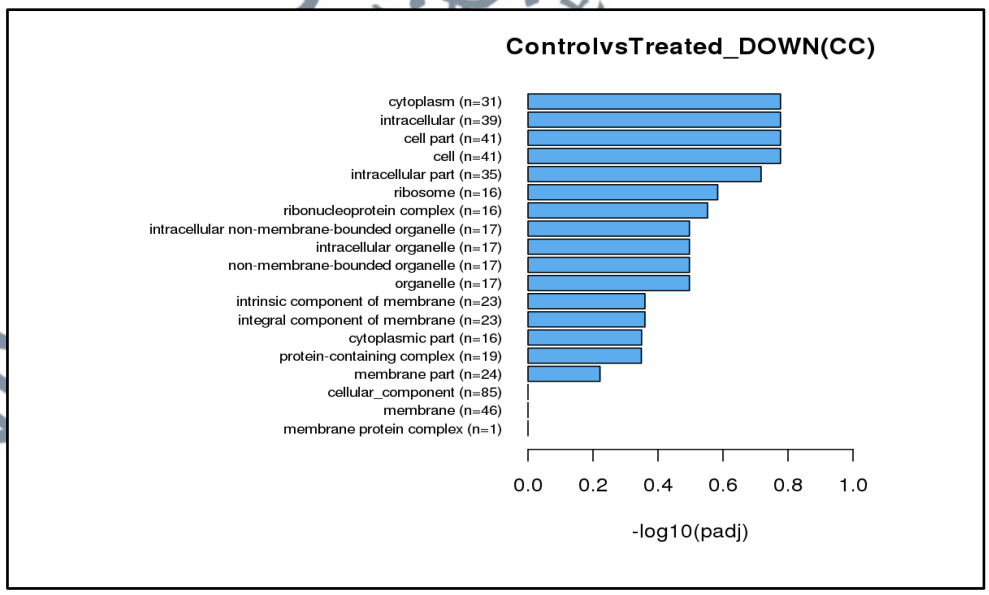

Figure 4.19: Gene Ontology Category of DEGs in Cellular Component.

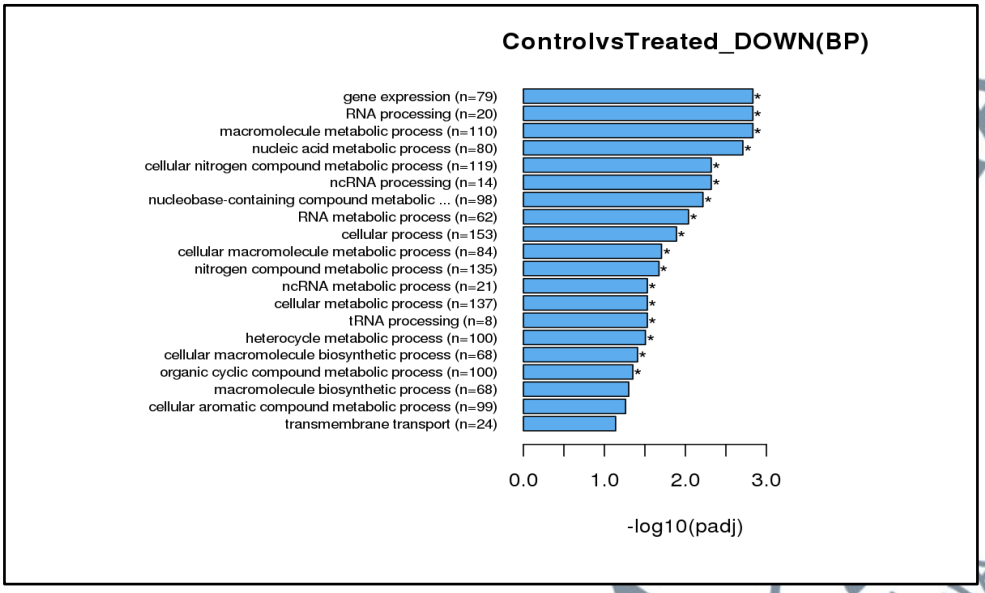

Figure 4.20: Gene Ontology Category of DEGs in Biology Process.

4.11.9 KEGG Pathway

Figure 4.21 and Figure 4.22 shows that the KEGG pathway of *S. mutans* were downregulated and upregulated, respectively after treatment with APFDE. *S. mutans* ribosome, DNA replication, peptidoglycan biosynthesis, and bacterial secretion system genes were all downregulated by the extract. Meanwhile, several pathways, including biosynthesis secondary metabolite, metabolic pathways, and fructose and mannose metabolism, are upregulated after APFDE exposure.

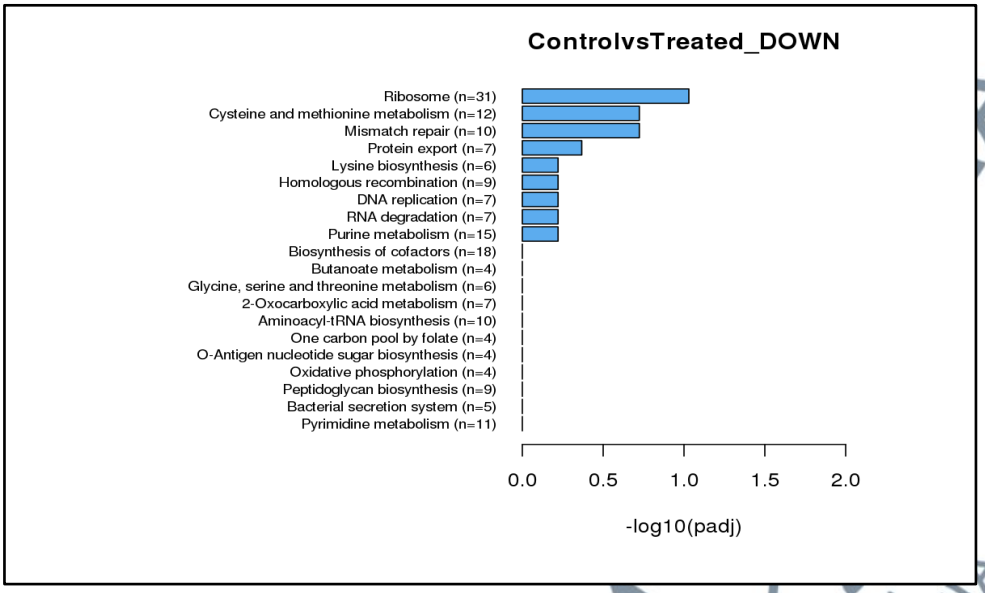

Figure 4.21: Downregulated of KEGG Pathway.

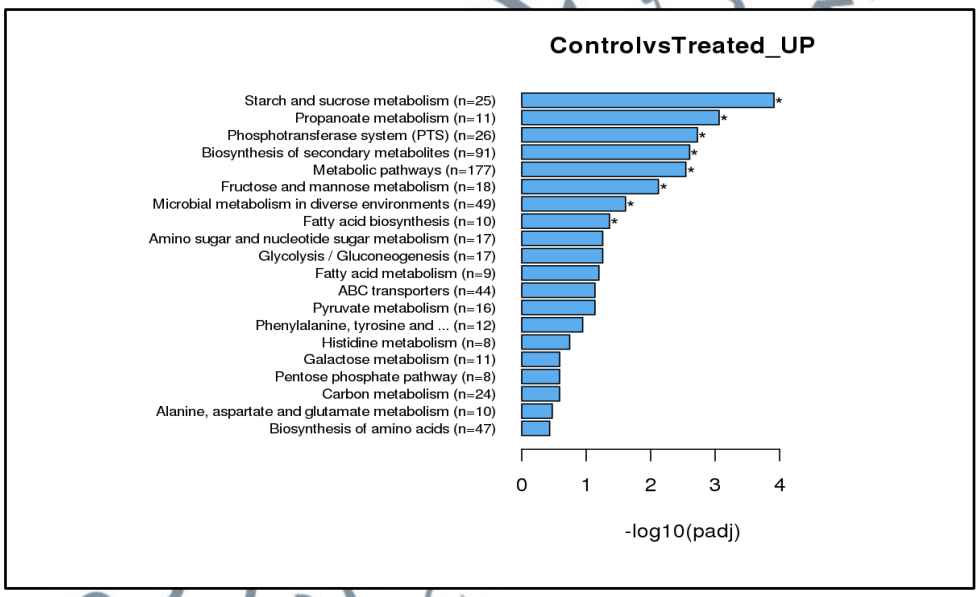

Figure 4.22: Upregulated of KEGG Pathway.

4.12 Novel Gene Prediction

The RNA-seq reads were assembled according to the reference genomes using Rockhopper (McClure et al., 2013), and then compared to known gene structures, so

that novel gene transcripts were predicted. The novel transcripts were aligned to sequences in NCBI NR database using Blast (cut-off: value < 1e-5). Novel transcripts with NR annotations were considered as novel potential protein coding transcripts. Table 4.11 showed the annotation of downregulated novels genes found in *S. mutans* after treated with extract. Several of novel genes was found in treated of *S. mutans* such as fatty acid metabolism, RNA degradation, ribosome, and biosynthesis of amino acids.

Table 4.11: The Annotation of Novel Genes in *S. mutans* After Treated with Extract (Downregulated).

Gene ID	Pathway Gene ID	Pathway ID	Pathway Name
Novel00007	SmuNN2025_0019	smc01230	Biosynthesis of amino acids
Novel00009	SmuNN2025_0062	smc02020	Two-component system
Novel00011	SmuNN2025_0092	smc01230	Biosynthesis of amino acids
Novel00012	SmuNN2025_0143	smc03010	Ribosome
Novel00016	SmuNN2025_0201	smc03018	RNA degradation
Novel00018	SmuNN2025_0263	smc02060	Phosphotransferase system (PTS)
Novel00019	SmuNN2025_0265	smc02060	Phosphotransferase system (PTS)
Novel00022	SmuNN2025_0312	smc00970	Aminoacyl-tRNA biosynthesis
Novel00023	SmuNN2025_0350	smc03070	Bacterial secretion system
Novel00034	SmuNN2025_0377	smc00061	Fatty acid biosynthesis
Novel00035	SmuNN2025_0379	smc01212	Fatty acid metabolism
Novel00036	SmuNN2025_0381	smc01212	Fatty acid metabolism
Novel00038	SmuNN2025_0432	smc00190	Oxidative phosphorylation